

Full Paper

Nondestructive measurement of sugar content of apple using hyperspectral imaging technique

Jiewen Zhao¹, Saritporn Vittayapadung^{1,*}, Quansheng Chen¹, Sumpun Chaitep² and Rachata Chuaviroj³

¹ School of Food and Biological Engineering, Jiangsu University, Zhenjiang, Jiangsu, 212013, P.R.China

² Faculty of Engineering, Chiang Mai University, Chiangmai, 50200, Thailand

³ Faculty of Engineering and Agro-Industry, Maejo University, Chiangmai, 50290, Thailand

* Corresponding author, e-mail: S_Vittayapadung@hotmail.com

Received: 14 March 2008 / Accepted: 25 March 2009 / Published: 30 March 2009

Abstract: Hyperspectral imaging technique is an upcoming and promising field of research for non-destructive quality assessment of agricultural and food products. It has a greater advantage of combining spatial imaging and spectral measurement which can detect both of the external and internal quality of the product. Sugar content is an important internal quality attribute for any fresh fruit. This research work focuses on evaluating the use of hyperspectral imaging technique which employs the wavelength range of 685-900 nm for detecting the quality of apple based on sugar content. The partial least square (PLS) method has the potential to produce the calibration and prediction model from their spectra. It was found that the optimal spectral range for sugar content of apple was 704.48-805.26 nm and the PLS calibration model for sugar content determination needed 4 PLS factors under standard normal variate (SNV) preprocessing method. The correlation coefficient (R) between the hyperspectral imaging prediction results and reference measurement results was equal to 0.90749. The PLS algorithm produced the calibration models which gave reasonably good correlation for estimating the sugar content of apple. It can thus be concluded that hyperspectral imaging technique is potentially useful for assessing sugar content of apple.

Keywords: hyperspectral imaging technique, apple, sugar content, PLS

Introduction

Non-destructive evaluation of the internal quality of fruits is an important field of research to improve their export potential. Determination of sugar content is a key factor to the export of fresh fruits. Sugar content is also one of the important parameters used for assessing apple quality. It may be determined from the juice extracted from the fruit flesh using refractometric method. However, this method of measurement is destructive, inefficient or time consuming, and prone to operational error. Unsuitable use of sugar content determination method for apple will result in less market value. The current method of apple sorting and grading for export market needs to be improved with more scientific approach. This issue can be addressed by evaluating the internal quality of the fruit non-destructively. Various researchers have reported on the development of different nondestructive sensing techniques for assessing postharvest quality of horticultural crops; they include mechanical force/deformation, sonic, impact, optical, and electrical techniques [1]. Most of these have not been adopted commercially because they do not correlate well with standard destructive measurements, nor meet the online sorting and grading requirements.

Exploring the possibility of using the optical property of fruits and vegetables for food product quality evaluation is gaining momentum. One example is near-infrared spectroscopy (NIRS), which has become a useful technique for measuring fruit internal quality, especially soluble solid content. Applications of NIRS have already been found for quality evaluation of food products, fruits and vegetables. Quality evaluation with the visible/near-infrared (VIS/NIR) region of spectra is being used to extract information from a small area or point from the food object. Considerable researches have reported on using NIRS to measure fruit internal quality such as sugar content or soluble solid content [2-8]. NIRS has also been demonstrated to have the potential for measuring other related flavour attributes for apple and other fruits [9-11]. Commercial NIRS systems are recently available for sorting and grading of fresh fruits. NIRS was also used for measuring fruit firmness [12-14] and other properties such as acidity [15-16]; however, the results are much less satisfactory. Also, NIRS is still unable to provide consistent and accurate measurement of other quality attributes such as fruit firmness [17-18]. Recently, hyperspectral or multispectral imaging technique was investigated for measuring fruit firmness and sugar content [19]. This new approach resulted in better prediction of fruit qualities than that by NIRS.

Hyperspectral imaging or imaging spectroscopy has its own advantage of extracting spectral information from a larger area of the object to provide more detailed information of the whole object. Application of this technique would be very useful for a more precise evaluation of internal properties of fruits. Lu and Peng [20] adopted the technique for predicting firmness of peach in the wavelength range of 500-1,000 nm. They found the best predictions at the wavelength of 677 nm for fruit firmness. Martinsen and Schaare [21] suggested 900-930 nm as important wavelength range for estimating soluble solid concentration of kiwi fruit. Dull et al. [22] selected 913 nm for predicting soluble solid content in sliced cantaloupe. Paliwal et al. [23] used different neural network models to classify cereal grains of five types based on their morphological character. The four-layer back-propagation network model classified the wheat and oat grains with satisfactory accuracy.

Noh and Lu [24] evaluated firmness and soluble solid content of Golden Delicious apple by hyperspectral reflectance scattering and fluorescence. Principle component analysis and neural network model were used for the prediction of firmness and soluble solid. Better prediction results were obtained with the model which combined both the fluorescence and reflectance value with a correlation of 0.75 and standard error of prediction of 6.97 N.

The objectives of this study are to evaluate another internal quality attribute, viz. sugar content based on the spectral information collected using a hyperspectral imaging system, to select the best wavelengths for the determination of sugar content, and to develop a prediction model for predicting these sugar content parameters of apples from their spectral information.

Materials and methods

Sample preparation

The fruit samples for the study were purchased from a local supermarket in Zhenjiang City of China. One hundred fruits of “Fuji” apple cultivar were used for the experiment. They were transported to the laboratory and were stored at room temperature (20 °C) for 3 hours before being measured. The apples were divided into two groups. The first group (60 apples) was used as the calibration set for building the calibration model, and the second group (40 apples) was used as the prediction set for testing the robustness of predictive models. Hyperspectral image acquisition and analysis was conducted on 4 positions at the opposite sides of each apple equator. After the image acquisition, the fruit was subjected to destructive analysis by the refractometer to determine the sugar content. All these analyses were done on peeled apples.

Hyperspectral imaging system and data acquisition

The hyperspectral image data were acquired through a hyperspectral imaging system, Figure 1(a), which was developed by the Agricultural Product Processing and Storage Laboratory at Jiangsu University. Figure 1(b) shows a sketch of the system consisting of a hyperspectral imaging camera set (with complementary metal oxide semiconductor (CMOS) camera, prism-grating-prism assembly, and C-mount lens), a motion controller, a motorised positioning table, fibre-optic illuminators, a light source, and a computer.

The whole system was divided into three modules: the sensor module, the lighting source module and the conveyer module. The sensor module was a Specim Hyperspectral Imaging Camera (ImSpector V10E, Specim Spectral Imaging Ltd., Oulu, Finland). It is an original equipment manufacturer (OEM) product which included a back-illuminated CMOS camera, a spectrograph with a prism-grating-prism construction and a C-mount lens which was attached to the CMOS camera. The spectral range was 408–1,117 nm with a nominal spectral resolution of 2.8 nm. For the lighting source module, two 150-W quartz-halogen DC stabilised fibre-optic illuminators (Fiber-Lite DC950 Illuminator, Dolan-Jenner Industries Inc, MA, USA) were used. The conveyer module consisted of an auto-translation stage or motorised positioning table (TSA200-A, Zolix Instruments Co., Ltd., Beijing, P.R. China) and a motion controller (SC300, Zolix Instruments Co., Ltd.). Thus, the motorised drive moves the lens assembly via the translation floor so that successive lines of the target are scanned while the target itself remains stationary.

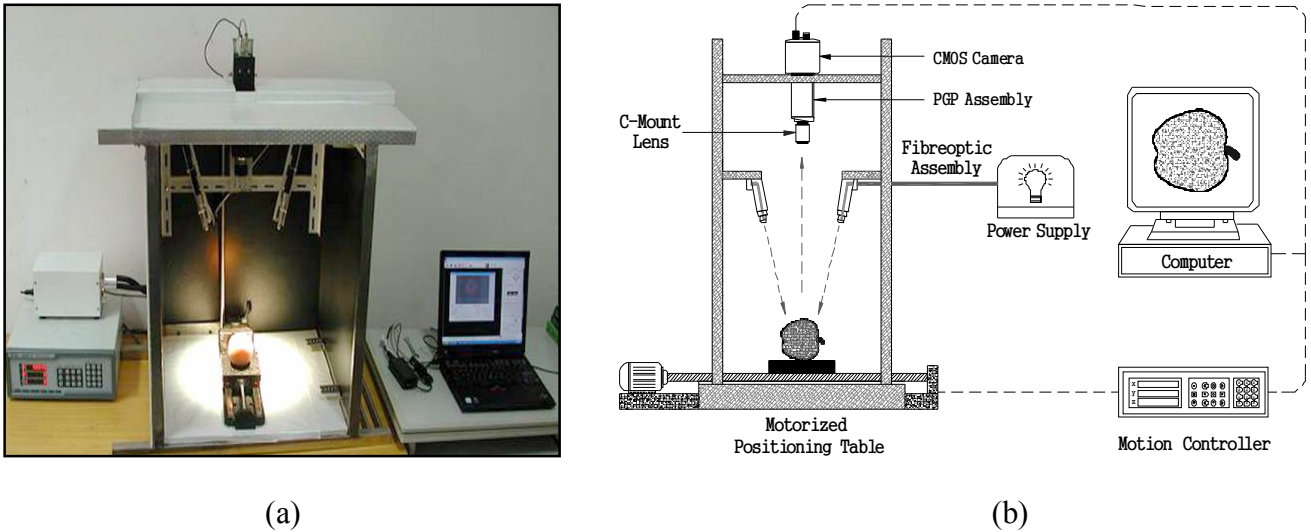


Figure 1. (a) Hyperspectral imaging system developed at the Agricultural Product Processing and Storage Laboratory, Jiangsu University, in Zhenjiang, P.R. China, (b) Sketch of the system

The apple sample was put on the platform of the translation floor and the acquisition of the hyperspectral imaging data was started. The hyperspectral imaging was captured line by line as the translation floor incrementally moved the samples through the field of view of the hyperspectral imaging camera under reflected light at wavelengths ranging from 408 nm to 1,117 nm with 0.67 nm intervals, which resulted in 1,024 spectral wavebands. The image data acquired by the hyperspectral imaging system were arranged with a spatial dimension of 1,280×600 pixels and with 1,024 spectral bands from 408 to 1,117 nm, as shown in Figure 2.

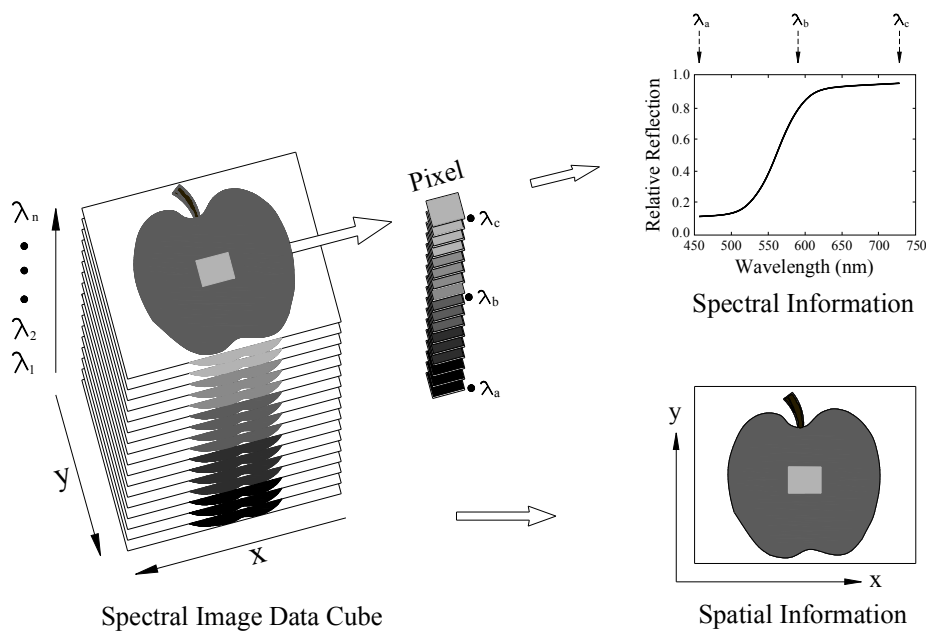


Figure 2. A three-dimension imaging cube (x, y, λ) acquired by the hyperspectral imaging system with two spatial dimensions (x, y) and one spectral dimension (λ)

Hyperspectral imaging data preprocessing

The hyperspectral images were firstly corrected with a white and a dark reference. The dark reference was used to remove the effect of the dark current of the CMOS detector, which is thermally sensitive [25-29]. The corrected image (R) was estimated using Eq. 1:

$$R = \frac{I - B}{W - B} \quad (1)$$

where I is the recorded hyperspectral image, B is the dark image (approximately 0% reflectance) recorded by turning off the lighting source with the lens of the camera completely closed, and W is the white reference imaging obtained by a white Spectralon panel (approximately 99% reflectance). Spectral reflectance R values range from 0 to 1.

The original spectral profile data of 100 apple samples are shown in Figure 3. In this research, spectral profiles of apple samples from 685-900 nm were used for analysis. Partial least square (PLS) algorithm of multivariate calibration was attempted several times to determine the optimal spectral range for constructing the calibration model. It was found that the optimal spectral range for sugar content of apples was 704.48-805.26 nm.

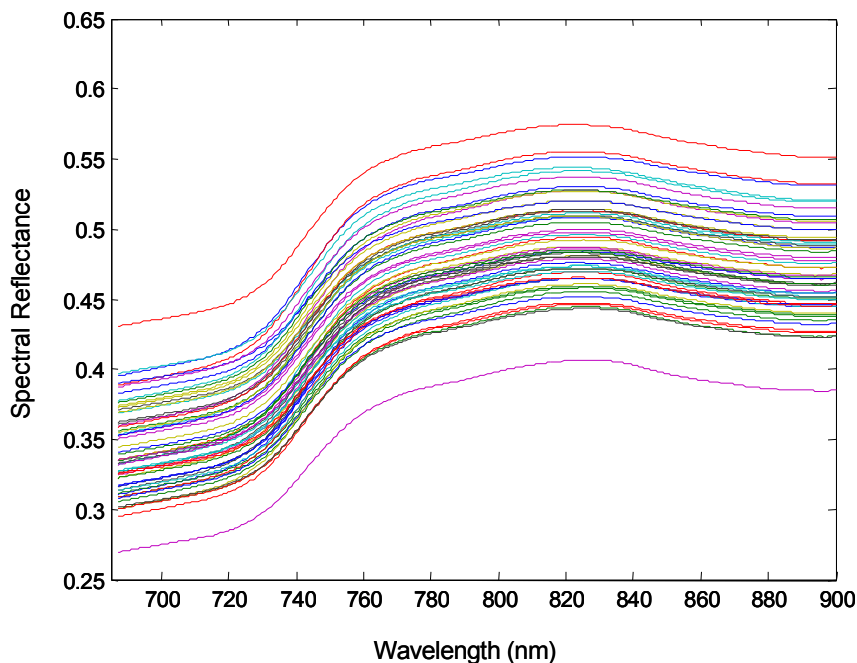


Figure 3. Original spectral profiles of apple samples from 685 nm to 900 nm

Sugar content reference measurement

A sugar refractometer (Model 2WA-J Abbe Refractometer, Shanghai Optical Instrument, China) reading in [$^{\circ}$ Brix] units with an accuracy of $\pm 0.2\%$ and a sugar content scale between 0-95% Brix was used for the determination of sugar content. A small sample of apple juice was used to measure the refractive index by the refractometer. The sugar content determination was performed on the same 4 positions as those used for hyperspectral imaging measurement on each apple sample around the equator. The mean value of sugar content was the average of 4 measurements.

Spectral preprocessing analysis

The spectral data were analysed using PLS regression with preprocessing. Four spectral preprocessing methods were applied comparatively: these were standard normal variate (SNV), mean centring, multiplicative scatter correction (MSC) and min/max normalisation.

First, SNV, a mathematical transformation method of the spectra, was used to remove slope variation and to correct for scatter effects. Each spectrum was corrected individually by first centring the spectral values, then, the centred spectrum was scaled by the standard deviation calculated from the individual spectral values. Second, the mean centring method process was to calculate the average spectrum of the data set and subtract that average from each spectrum. Third, MSC was used for the correction of scattered light on the basis of different particle sizes. The technique was used for correcting the additive and multiplicative effects in the spectra. Finally, min/max normalisation, a type of normalisation, was utilised to transform the data into a preferred range, in which the minimum value of an attribute was subtracted from each value of the attribute and then the difference divided by the range of the attribute [30-31]. In general, the range of the spectral value after min/max normalisation spectral preprocessing is set [0 1]. Figure 4 shows the results of the different methods after preprocessing.

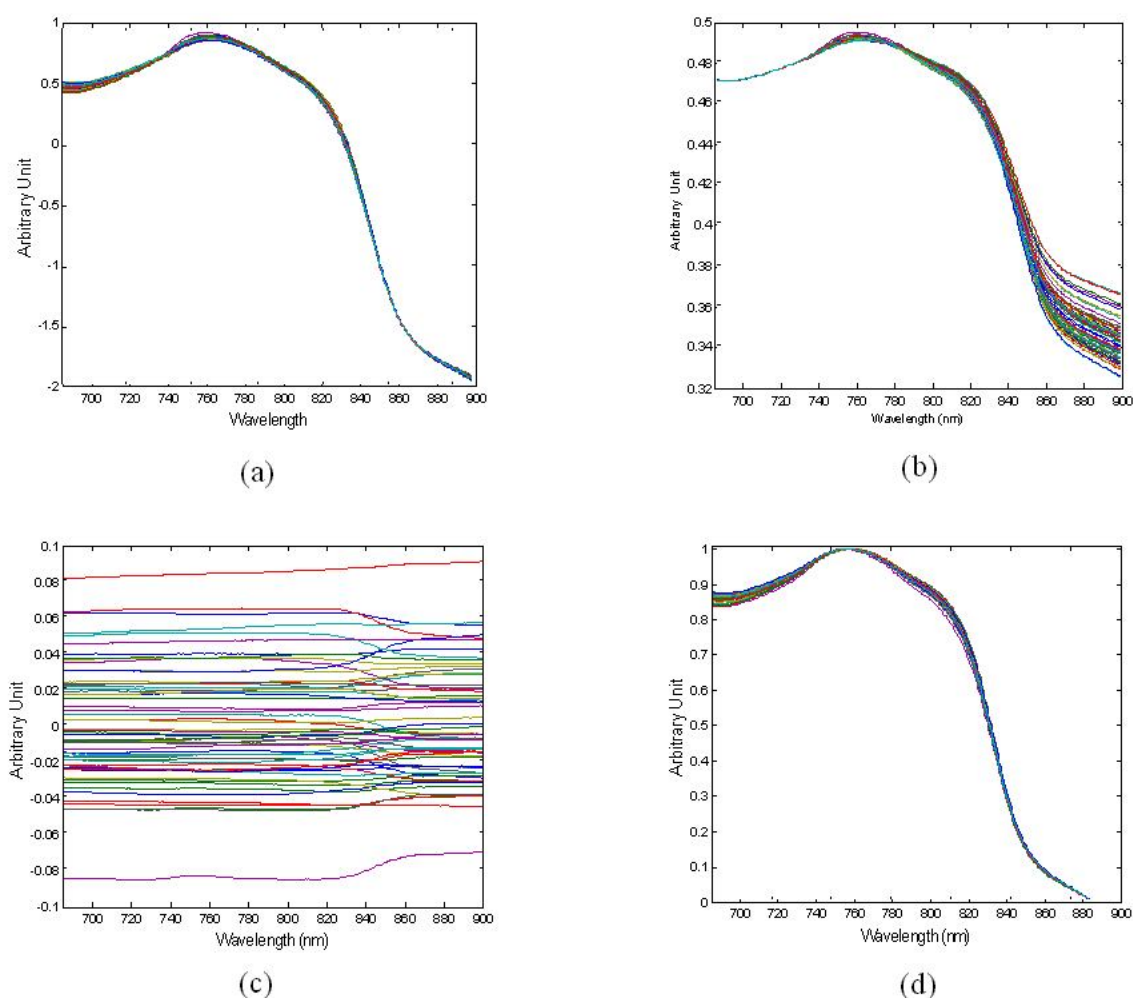


Figure 4. Preprocessing reflectance spectra of apples: (a) SNV, (b) MSC, (c) mean centring, and (d) min/max normalisation

Software

For the hyperspectral imaging data acquisition, Spectral Cube (Spectral Imaging Ltd., Finland, AutoVision Inc., CA, USA) was used. All data processing and analysis were performed with environment for visualising images (ENVI) V.4.3 (Research Systems Inc., Boulder Co., USA) and Matlab Version.7.0 (Mathworks, Natick, USA) for Windows XP.

Results and Discussion

Quantitative analysis of the PLS model

One hundred “Fuji” apples were selected to construct the PLS model in this experiment. All 100 spectra were divided into 2 sets, i.e. the calibration set and the prediction set. To avoid bias in the subset selection, the division was arranged as follows: all samples were sorted according to their respective y-value, viz. the reference measurement value of sugar content. In order to come to a 3/2 division of calibration/prediction spectra, three spectra from every five samples were selected for the calibration set, and two for the prediction set so that finally the calibration set contained 60 spectra (Table 1). The remaining 40 spectra constituted the prediction set (Table 2). As seen in Tables 1 and 2, the range of y values in the calibration set covers that in the test set, therefore the distribution of the samples was appropriate in the calibration and prediction sets.

Table 1. Reference measurements and sample numbers in calibration set

Component	Unit	S.N.	Range	Mean	S.D.
Sugar content	°Brix	60	7.20-17.45	12.50	1.75

S.N. = sample number; S.D. = standard deviation, °Brix = sugar content unit

Table 2. Reference measurements and sample numbers in prediction set

Component	Unit	S.N.	Range	Mean	S.D.
Sugar content	°Brix	40	8.52-15.60	12.51	1.61

S.N. = sample number; S.D. = standard deviation, °Brix = sugar content unit

The performance of the final PLS model was evaluated in terms of the root mean square error of cross-validation (RMSECV), the root mean square error of prediction (RMSEP), and the correlation coefficient (R). For RMSECV, a leave-one-sample-out cross-validation was performed: the spectrum of one sample of the calibration set was deleted from this set and a PLS model was built with the remaining spectra of the prediction set [32]. The left-out sample was predicted with this model and the procedure was repeated by leaving out each of the samples of the calibration set. RMSECV was calculated according to Eq.2:

$$RMSECV = \sqrt{\frac{\sum_{i=1}^n \left(\hat{y}_i - y_i \right)^2}{n}} \quad (2)$$

where n is the number of samples in the calibration set, y_i is the reference measurement result for sample i , and \hat{y}_i is the estimated result for sample i when the model is constructed with sample i removed. The number of PLS factors included in the model was chosen according to the lowest RMSECV. This procedure was repeated for each of the preprocessed spectra. For the prediction set, RMSEP was calculated according to Eq. 3:

$$RMSEP = \sqrt{\frac{\sum_{i=1}^n (y_i - \hat{y}_i)^2}{n}} \quad (3)$$

where n is the number of apple samples in the prediction set, y_i is the reference measurement result for prediction set sample i , and \hat{y}_i is the estimated result of the model for prediction sample i . Finally, the model with the overall lowest RMSECV was selected as the final model. Correlation coefficients between the predicted and the measured value were calculated for both the training and the test set according to Eq. 4:

$$R = \sqrt{1 - \frac{\sum_{i=1}^n (\hat{y}_i - y_i)^2}{\sum_{i=1}^n (y_i - \bar{y}_i)^2}} \quad (4)$$

Sugar content

In the application of PLS algorithm, it is generally known that the spectral preprocessing methods and the number of PLS factors are deciding parameters. The optimum number of factors is determined by the lowest RMSECV. Figure 5 shows the RMSECV plotted as a function of PLS factors for determining the sugar content with different spectral preprocessing methods, i.e. SNV, MSC, mean centring and min/max normalisation. It was found that the RMSECV of SNV and min/max method decreased sharply together in the same trend, while the RMSECV of MSC and mean centring method were higher than the former.

However, in comparing between the four spectral preprocessing methods, it was found that the SNV spectral preprocessing method exhibited the best result, and when the number of principal components (PCs) was equal to 4, the value of RMSECV was lowest. Therefore, the best predictive model was achieved with 4 PLS factors after the SNV spectral preprocessing method.

Table 3 shows the best results of the calibration models by different spectral preprocessing methods for determining sugar content. Apparently, the lowest RMSECV, equal to 0.70699 °Brix, was obtained with the SNV spectral preprocessing method, which needed 4 PLS factors. In this application then, the SNV seemed to perform better than other preprocessing methods.

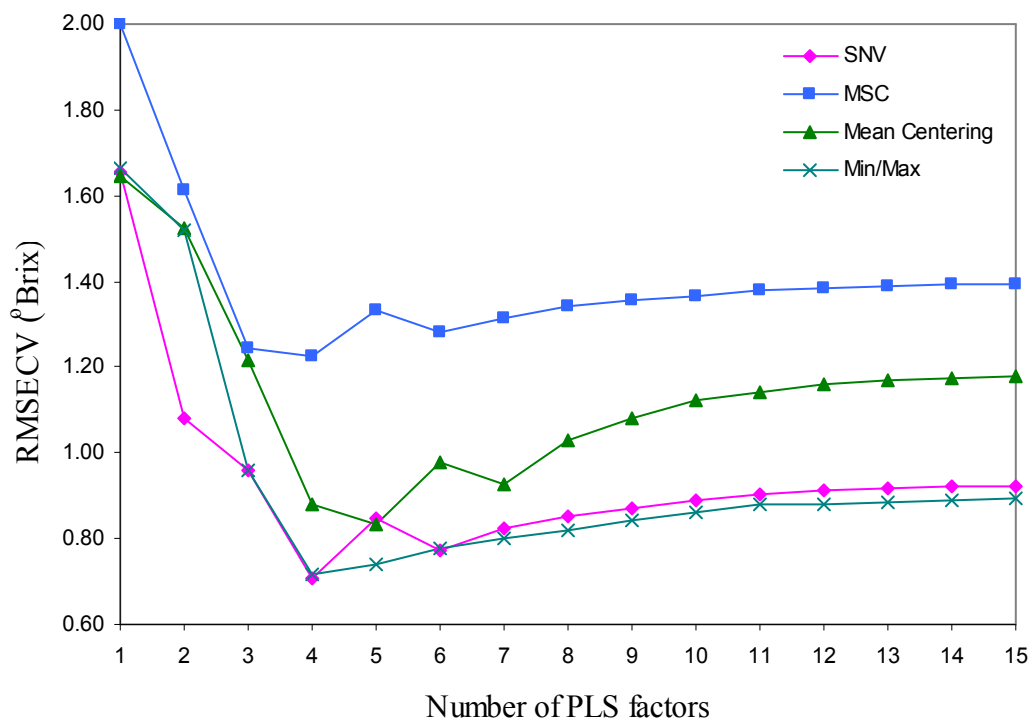


Figure 5. Effect of number of PLS factors on RMSECV for sugar content calibration model

Table 3. Best results for each of the processing method for the models of sugar content

Preprocessing method	PLS factors	RMSECV (°Brix)	RMSEP (°Brix)	R (calibration)	R (prediction)
SNV	4	0.70699	0.66942	0.89771	0.90749
MSC	4	1.22370	0.90198	0.64691	0.82438
Mean centring	5	0.83328	0.85155	0.85461	0.84525
Min/max normalisation	4	0.71608	0.67512	0.88946	0.90029

Figure 6 gives a scatter plot showing a correlation between hyperspectral imaging prediction value and reference measurement of sugar content by the SNV spectral preprocessing method. All blue dots represent prediction data, which are in good correlation with the reference measurement data; many points fall on or close to the unity line. Sugar content in the prediction set was predicted with the RMSEP value of 0.66942 °Brix. The correlation coefficients for this calibration model are equal to 0.89771 and 0.90749 for the calibration and prediction set respectively.

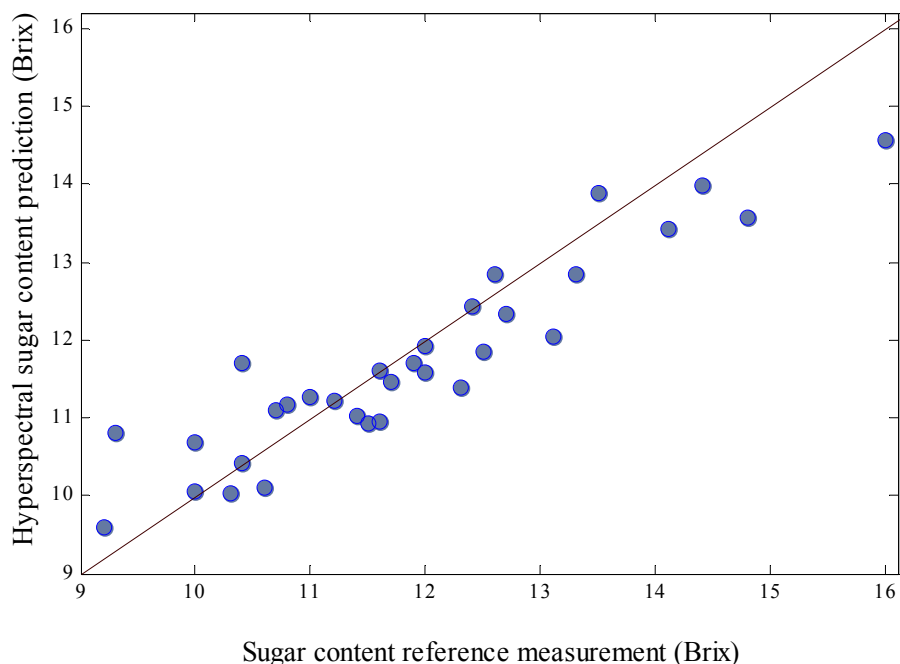


Figure 6. Reference determinations versus hyperspectral prediction for sugar content of calibration set data

Conclusions

The study has shown the potential application of hyperspectral imaging technique for the prediction of sugar content of apple fruits. The technique employed the wavelength range of 685-900 nm for estimating the sugar content. It was found that the optimal spectral range for sugar content of apples was 704.48-805.26 nm. The PLS method has the potential to estimate the calibration and prediction model from their spectra. The PLS calibration model for sugar content determination was found to need 4 PLS factors under the SNV preprocessing method. The correlation coefficient (R) between the hyperspectral imaging prediction results and the reference measurement results was equal to 0.90749. The PLS algorithm produced the calibration models which gave a reasonably good correlation for estimating the sugar content of apple.

Acknowledgements

This work was financially supported by the Key Natural Science Foundation of Jiangsu Province (Grant No. BK2006707-1) and the National High Technology Research and Development Program of China (863 Project, No. 2006AA10Z263). We also wish to thank many of their academic colleagues for stimulating discussions in this field.

References

1. J. A. Abbott, R. F. Lu, B. L. Upchurch, and R. L. Stroshine, "Technologies for nondestructive quality evaluation of fruits and vegetables", in *Horticultural Reviews*, Volume 20 (Ed. J. Janick), John Wiley and Sons, New York, **1997**, pp.1-120.
2. R. F. Lu and D. Ariana, "A near-infrared sensing technique for measuring internal quality of apple fruit", *Appl. Eng. Agric.*, **2002**, *18*, 585-590.
3. R. F. Lu, "Imaging spectroscopy for assessing internal quality of apple fruit", Mich: ASAE, St. Joseph, ASAE Paper No.036012, **2003**.
4. D. Ariana, B. P. Shrestha, and D. E. Guyer, "Integrating reflectance and fluorescence imaging for apple disorder classification", Mich: ASAE, St. Joseph, ASAE Paper No. 033120, **2003**.
5. V. Smail, A. Fritz, and D. Wetzel, "Chemical imaging of intact seeds with NIR focal plane array assists plant breeding", *Vib. Spectrosc.*, **2006**, *42*, 215-221.
6. O. Rodionova, L. Houmoller, A. Pomerantsev, P. Geladi, J. Burger, V. Dorofeyev, and A. Arzamastsev, "NIR spectrometry for counterfeit drug detection: A feasibility study", *Anal. Chim. Acta*, **2005**, *549*, 151-158.
7. Y. Roggo, A. Edmond, P. Chalus, and M. Ulmschneider, "Infrared hyperspectral imaging for qualitative analysis of pharmaceutical solid forms", *Anal. Chim. Acta*, **2005**, *535*, 79-87.
8. G. Zheng, Y. Chen, X. Intes, B. Chance, and J. D. Glickson, "Contrast enhanced near-infrared (NIR) optical imaging for subsurface cancer detection", *J. Porphyrins Phthalocyanines*, **2004**, *8*, 1106-1117.
9. D. K. Lovett, E. R. Deaville, D. I. Givens, M. Finlay, and E. Owen, "Near infrared reflectance spectroscopy (NIRS) to predict biological parameters of maize silage: effects of particle comminution, oven drying temperature and the presence of residual moisture", *Anim. Feed Sci. Technol.*, **2005**, *120*, 323-332.
10. S. Kang, K. J. Lee, W. Choi, L. R. Son, D. S. Choi, and G. Kim, "A near infrared sensing technique for measuring the quality of potatoes", Mich: ASAE, St. Joseph, ASAE Paper No: 033137, **2004**.
11. S. Saranwong, J. Sornsrivichai, and S. Kawano, "Prediction of ripe-stage eating quality of mango fruit from its harvest quality measured nondestructively by near infrared spectroscopy", *Postharvest Biol. Technol.*, **2004**, *31*, 137-145.
12. R. F. Lu and Y. K. Peng, "Hyperspectral scattering for assessing peach fruit firmness", Mich: ASAE, St. Joseph, ASAE Paper No. 043007, **2004**.
13. J. Lammertyn, B. Nicolai, K. Ooms, V. De Smedt, and J. De Baerdemaeker, "Nondestructive measurement of acidity, soluble solids, and firmness of Jonagold apples using NIR-spectroscopy", *Trans. ASAE*, **1998**, *41*, 1089-1094.
14. V. A. McGlone, R. B. Jordan, and P. J. Martinsen, "VIS/NIR estimation at harvest of pre- and post-storage quality indices for 'Royal Gala' apple", *Postharvest Biol. Technol.*, **2002**, *25*, 135-144.

15. G. Downey and J. D. Kelly, "Detection and quantification of apple adulteration in diluted and sulfited strawberry and raspberry purees using visible and near-infrared spectroscopy", *J. Agric. Food Chem.*, **2004**, 52, 204-209.
16. Z. Schmilovitch, A. Mizrach, A. Hoffman, H. Egozi, and Y. Fuchs, "Determination of mango physiological indices by near-infrared spectrometry" *Postharvest Biol. Technol.*, **2000**, 19, 245-252.
17. V. A. McGlone and S. Kawano, "Firmness, dry-matter and soluble-solids assessment of postharvest kiwifruit by NIR spectroscopy", *Postharvest Biol. Technol.*, **1998**, 13, 131-141.
18. R. F. Lu, D. E. Guyer, and R. M. Beaudry, "Determination of firmness and sugar content of apples using near-infrared diffuse reflectance", *J. Texture Stud.*, **2000**, 31, 615-630.
19. G. Polder, W. A. M. Van Der Heijden, and I. T. Young, "Spectral image analysis for measuring ripeness of tomatoes", *Trans. ASAE*, **2002**, 45, 1155-1161.
20. R. F. Lu and Y. K. Peng, "Hyperspectral scattering for assessing peach fruit firmness", *Biosystems Eng.*, **2006**, 93, 161-171.
21. P. Martinsen and P. Schaare, "Measuring soluble solids distribution in kiwifruit using near infrared imaging spectroscopy", *Postharvest Biol. Technol.*, **1998**, 14, 271-281.
22. G. G. Dull, S. B. Gerald, A. S. Doyle, and G. L. Richard, "Near infrared analysis of soluble solids in intact cantaloupe", *J. Food Sci.*, **1989**, 54, 393-395.
23. J. Paliwal, N. S. Visen, and D. S. Jayas, "Evaluation of neural network architectures for cereal grain classification using morphological features", *J. Agric. Eng. Res.*, **2001**, 79, 361-370.
24. H. K. Noh and R. F. Lu. "Hyperspectral reflectance and fluorescence for assessing apple quality", Mich: ASAE, St. Joseph, ASAE Paper No. 053069, **2005**.
25. E. Hege, D. O'Connell, W. Johnson, S. Basty, and E. Dereniak, "Hyperspectral imaging for astronomy and space surveillance", *Proc. SPIE 5159*, **2003**, 380-391.
26. D. Kellicut, J. Weiswasser, S. Arora, J. Freeman, R. Lew, C. Shuman, J. Mansfield, and A. Sidawy, "Emerging technology: Hyperspectral imaging", *Perspect. Vasc. Surg.*, **2004**, 16, 53-57.
27. J. Qiao, M. O. Ngadi, W. Ning, C. Gariepy, and S. O. Prasher, "Pork quality and marbling level assessment using a hyperspectral imaging system", *J. Food Eng.*, **2007**, 83, 10-16.
28. J. Qiao, N. Wang, M. O. Ngadi, A. Gunenc, M. Monroy, C. Gariepy, and S. O. Prasher, "Prediction of drip-loss, pH, and color for pork using a hyperspectral imaging technique", *Meat Sci.*, **2007**, 76, 1-8.
29. B. Park, W. R. Windham, K. C. Lawrence, and D. P. Smith, "Contaminant classification of poultry hyperspectral imagery using a spectral angle mapper algorithm", *Biosystems Eng.*, **2007**, 96, 323-333.
30. Q. S. Chen, J. W. Zhao, X. Y. Huang, H. D. Zhang, and M. H. Liu, "Simultaneous determination of total polyphenols and caffeine contents of green tea by near-infrared reflectance spectroscopy", *Microchem. J.*, **2006**, 83, 42-47.
31. S. Vittayapadung, J. W. Zhao, Q. S. Chen, and R. Chuaviroj, "Application of FT-NIR spectroscopy to the measurement of fruit firmness of "Fuji" apples", *Maejo Int. J. Sci. Technol.*, **2008**, 2, 13-23.

Maejo Int. J. Sci. Technol. **2009**, 3(01), 130-142

32. Q. S. Chen, J. W. Zhao, H. D. Zhang, and X. Y. Wang, "Feasibility study on quality and quantitative analysis in tea by near infrared spectroscopy with multivariate calibration", *Anal. Chim. Acta*, **2006**, 572, 77-81.

© 2009 by Maejo University, San Sai, Chiang Mai, 50290 Thailand. Reproduction is permitted for noncommercial purposes.